

Intermittent hypoxia-induced enhancements in corticospinal excitability predict gains in motor learning and metabolic efficiency

Alysha T. Bogard

University of Colorado Boulder

Thomas G. Hembree

University of Colorado Boulder

Aviva K. Pollet

University of Colorado Boulder

Andrew C. Smith

University of Colorado Anschutz Medical Campus

Stephanie C. Ryder

Rocky Mountain Regional VA Medical Center

George E. Marzloff

Rocky Mountain Regional VA Medical Center

Andrew Quesada Tan

`andrew.tan@colorado.edu`

University of Colorado Boulder

Article

Keywords:

Posted Date: April 24th, 2024

DOI: <https://doi.org/10.21203/rs.3.rs-4259378/v1>

License:   This work is licensed under a Creative Commons Attribution 4.0 International License.

[Read Full License](#)

Additional Declarations: No competing interests reported.

Intermittent Hypoxia-Induced Enhancements in Corticospinal Excitability Predict Gains in Motor Learning and Metabolic Efficiency

Alysha T. Bogard¹, Thomas G. Hembree¹, Aviva K. Pollet¹, Andrew C. Smith²,
Stephanie C. Ryder³, George Marzloff³, and Andrew Q. Tan^{*1,3,4}

¹*Sensorimotor Recovery and Neuroplasticity Lab at the University of Colorado, Boulder, Dept. of Integrative Physiology, 80309, USA*

²*University of Colorado School of Medicine, Dept. of Physical Medicine and Rehabilitation, Aurora, 80045, USA*

³*Rocky Mountain Regional VA Medical Center, Aurora, 80045, USA*

⁴*Center for Neuroscience, University of Colorado, Boulder, 80309, USA*

**Corresponding Author: andrew.tan@colorado.edu*

ABSTRACT

Acute intermittent hypoxia (AIH) enhances human motor function after incomplete spinal cord injury. Although the underlying mechanisms in humans are unknown, emerging evidence indicates that AIH facilitates corticospinal excitability to the upper limb. However, the functional relevance of this plasticity remains unexplored, and it is unclear whether similar plasticity can be induced for lower limb motor areas. We recently demonstrated that AIH improves motor learning and metabolic efficiency during split-belt walking. Thus, we hypothesized that AIH increases lower limb excitability and that these enhancements would predict the magnitude of motor learning and the corresponding reductions in net metabolic power. We assessed tibialis anterior (TA) excitability using transcranial magnetic stimulation and quantified changes in spatiotemporal asymmetries and net metabolic power in response to split-belt speed perturbations. We show that AIH enhances TA excitability, and that the magnitude of this facilitation positively correlates with greater spatiotemporal adaptation. Notably, we demonstrate a novel association between increased excitability and reduced net metabolic power during motor learning and savings. Together, our results suggest that AIH-induced gains in excitability predict both the magnitude of motor learning and the associated metabolic efficiency. Determining indices of AIH-induced improvements in motor performance is critical for optimizing its therapeutic reach.

Introduction

Acute intermittent hypoxia (AIH), involving brief alternating exposures to low-oxygen air, shows promise as an adjuvant to conventional locomotor training to enhance motor function following a motor incomplete spinal cord injury (iSCI)^{1–3}. Despite considerable research in rodents^{4,5}, the neural mechanisms underlying gains in motor performance remain unclear in humans. Both animal⁶ and human studies⁷ suggest that AIH induces neuroplastic changes that prime the nervous system for further improvements in motor function with neurorehabilitation training. Understanding the neurophysiological underpinnings of AIH-induced plasticity and its functional significance is critical to optimize its therapeutic reach.

One potential mechanism underlying AIH-induced gains in motor performance is enhanced excitability of residual descending motor pathways. Motor-evoked potentials (MEPs) elicited by transcranial magnetic stimulation (TMS) reflect the net excitability of intracortical and transcortical networks synapsing onto corticospinal neurons⁸. Previous studies in able-bodied individuals have shown that AIH may facilitate corticospinal excitability (CSE) to the upper limb^{9,10}. However, contrasting evidence indicates that prolonged hypoxic exposures do not alter CSE¹¹, and even milder exposures result in inconsistencies in both the time course and stimulus intensity required for such augmentation^{9,10}. These discrepancies underscore a critical gap in our understanding of AIH-induced plasticity, including uncertainties regarding how AIH may differentially affect lower limb motor areas that support locomotor control. Furthermore, it remains unclear how increased CSE influences motor performance.

Our recent study demonstrated that AIH enhances spatiotemporal adaptation during a novel split-belt walking task, suggesting that AIH may mediate motor performance through processes involved in motor learning¹². Such enhancements may be attributed to brain-derived neurotrophic factor (BDNF)-dependent mechanisms known to enhance both CSE and motor learning^{13,14}. Evidence from rodent models indicates that moderate AIH exposures increase motoneuron excitability through BDNF-dependent mechanisms^{4,5}. Therefore, AIH-induced enhancements in CSE may not only reflect the net changes in excitability but also subserve gains in motor learning.

Converging evidence from human studies reports positive correlations between elevated CSE and enhanced motor learning^{15,16}. Gains in CSE may relate to the challenge of the motor learning process itself¹⁷ rather than specific movement parameters¹⁸. Notably, tibialis anterior (TA) excitability increases after novel skill training but not after repetitive movement training¹⁹. Moreover, TA excitability is amplified during late stance of a precision target-matching walking task relative to regular walking²⁰. Conversely, disrupting motor cortical processing through repetitive stimulation subsequently lowers CSE and impedes motor retention²¹. Together, this evidence suggests that elevated CSE may serve as a marker of neuroplastic processes that promote motor learning.

Accordingly, this study investigated the effects of five consecutive days of AIH on TA excitability and motor learning. AIH involved 90-second intervals of breathing 9% \pm 2% O₂ alternated with 60-second intervals of 21% \pm 2% O₂ for 15 cycles³. We measured changes in resting TA excitability pre-AIH and post-AIH using single-pulse TMS. To assess whether AIH-induced enhancements in CSE influence motor learning without any prior training, participants performed a split-belt walking task after the final AIH dose to eliminate the confound of task familiarity¹².

We hypothesized that AIH would increase TA excitability and that the magnitude of change would predict the extent of spatiotemporal adaptation during split-belt walking. Since greater spatiotemporal adaptation is associated with decreased metabolic power²², with more pronounced reductions after AIH¹², we further predicted a positive correlation between increased TA excitability and reduced net metabolic power. Bridging the gap between AIH-induced neuroplasticity and its functional significance is critical for maximizing the neurorehabilitative benefits of AIH.

Results

AIH Increases Lower Limb Excitability

Thirteen able-bodied subjects participated in a within-subjects design to assess changes in CSE after 5 consecutive days of AIH. We generated recruitment curves by plotting the peak-to-peak MEP amplitudes against the normalized stimulus intensities based on the participant's resting motor threshold (RMT) (Fig. 1)¹¹. To assess changes in CSE, we

quantified TMS indices such as changes in the maximum MEP amplitude (MEP_{max}), the area under the recruitment curve, the peak slope of the recruitment curve, and RMT.

We observed a significant increase in TA excitability after AIH (Fig. 2), as shown by significant enhancements in both MEP_{max} ($W = 14$, $p = 0.027$) and the area under the recruitment curve ($W = 13$, $p = 0.021$). Additionally, we observed a decrease in RMT after AIH, indicating a lower threshold to excite the TA; however, this change only approached significance ($W = 44.5$, $p = 0.088$). In contrast, peak slope ($W = 25$, $p = 0.168$) and maximal voluntary contraction ($t(12) = -0.78$, $p = 0.450$) did not change after AIH.

Furthermore, a repeated measures ANOVA comparing the MEP amplitude pre-AIH and post-AIH at the stimulus intensities of 100% RMT, 120% RMT, and 140% RMT, showed a significant main effect of both timepoint ($F(1, 12) = 6.66$, $p = 0.024$) and stimulus intensity ($F(1.18, 14.19) = 36.29$, $p < 0.001$) on MEP amplitude, as well as a significant interaction between timepoint and stimulus intensity ($F(1.49, 17.86) = 4.79$, $p = 0.030$). Tukey's post-hoc comparisons indicated a significant increase in MEP amplitude from pre- to post-AIH for the stimulus intensities of 120% RMT ($t(12) = -2.18$, $p = 0.050$) and 140% RMT ($t(12) = -2.75$, $p = 0.018$). These findings collectively demonstrate that five consecutive days of AIH significantly enhanced TA excitability.

Background EMG

To ensure stable levels of pre-stimulus muscle activation, we compared the mean background EMG recorded 200 ms preceding the TMS stimuli²³. We did not observe any statistically significant differences in background EMG activity between pre-TMS and post-TMS sessions ($t(12) = -0.72$, $p = 0.486$). This observation indicates that the variability in background EMG is not a significant factor contributing to any observed changes in the TA MEP amplitude pre- to post-AIH.

Motor Learning: Spatiotemporal Asymmetry

We assessed motor learning by quantifying the extent of spatiotemporal adaptation from the first five strides ('initial learning') to the last twenty strides ('late learning') of two, 300-stride split-belt walking conditions, Adapt 1 and Adapt 2 (Fig. 3A-C). For both adaptation conditions, the perturbation was set at a 2:1 belt speed ratio. The spatiotemporal

parameters of motor learning we analyzed included step length asymmetry (SLA), step time asymmetry (STA), and double support time asymmetry (DSA). Values that converged with the adaptation patterns extensively observed in able-bodied individuals reflected greater 'learning.' Specifically, we characterized motor learning by reductions in SLA and DSA towards symmetry values of 0, coupled with increases in STA towards positive asymmetry^{24,25}. One participant was excluded from all gait analyses due to utilizing a running strategy with a distinct aerial phase.

We found that participants adapted their interlimb coordination during Adapt 1 and Adapt 2 to minimize SLA and DSA, while maintaining an increased STA. A two-way ANOVA revealed significant main effects of both condition ($F(1, 11) = 22.99, p < 0.001$) and learning phase ($F(1, 11) = 36.15, p < 0.001$) on SLA, with a significant interaction between condition and learning phase ($F(1,11) = 15.43, p = 0.002$). Tukey's post-hoc comparisons demonstrated a significant decrease in SLA from initial Adapt 1 to late Adapt 1 ($t(11) = -5.65, p < 0.001$) and from initial Adapt 2 to late Adapt 2 ($t(11) = -4.73, p < 0.001$). Conversely, for STA, a two-way ANOVA only observed a significant main effect of condition ($F(1, 11) = 7.78, p = 0.018$). However, Tukey's post-hoc comparisons did not indicate any significant changes in STA between initial Adapt 1 to late Adapt 1 ($p = 0.214$), nor between initial Adapt 2 to late Adapt 2 ($p = 0.784$). For DSA, a two-way ANOVA showed significant main effects of condition ($F(1, 11) = 38.79, p < 0.001$) and learning phase ($F(1, 11) = 14.89, p = 0.003$), with a significant interaction between the two ($F(1, 11) = 6.82, p = 0.024$). Tukey's post-hoc comparisons indicated a significant decrease in DSA from initial to late Adapt 1 ($t(11) = -4.16, p = 0.002$) and initial to late Adapt 2 ($t(11) = 2.21, p = 0.049$). These observations underscore the ability of able-bodied individuals to bilaterally adapt spatial and temporal interlimb coordination in response to the imposed belt speed perturbations.

Motor Learning: Net Metabolic Power

Given that spatiotemporal adaptations are paralleled by reductions in metabolic cost during split-belt walking^{12,22}, we quantified concurrent changes in net metabolic power (W/kg) utilizing open-circuit spirometry. To account for the time lag of expired air reaching

the mixing chamber, we quantified changes in 'early' and 'late' net metabolic power during the second and last minute of each condition, respectively (Fig. 3D)²².

An ANOVA detected significant main effects of condition ($F(1, 11) = 9.76$, $p = 0.010$) and an interaction effect between condition and learning phase ($F(1, 11) = 17.60$, $p = 0.001$). Tukey's post-hoc comparisons identified a significant decrease in net metabolic power from early to late Adapt 1 ($t(11) = 3.90$, $p = 0.002$) and from early to late Adapt 2 ($t(11) = -2.47$, $p = 0.031$). Mean net metabolic power decreased from 6.09 W/kg during early Adapt 1 ($SE = 0.44$) to 5.73 W/kg during late Adapt 1 ($SE = 0.38$). Thus, as participants adapted their coordination, they simultaneously improved their metabolic efficiency.

Lower Limb Excitability Predicts Motor Learning: Spatiotemporal Asymmetry

We performed linear regression analyses and calculated the adjusted R^2 values to evaluate how well ΔMEP_{max} , Δ area under the recruitment curve, Δ peak slope, and Δ RMT predicted the magnitude of motor learning (Fig. 4, Table 1). We observed a significant positive correlation between increased MEP_{max} after AIH and reduced SLA during motor learning (Adjusted $R^2 = 0.418$, $p = 0.014$). Moreover, a positive trend emerged between elevated area under the recruitment curve after AIH and decreased SLA during motor learning (Adjusted $R^2 = 0.256$, $p = 0.053$). Stepwise linear regression identified both ΔMEP_{max} and Δ peak slope as the primary predictors of improved SLA during motor learning ($\Delta SLA = 0.097 + 0.420 * \Delta MEP_{max} - 0.423 * \Delta$ peak slope, $AIC = -65.29$, model $p = 0.039$, MEP_{max} $p = 0.032$, peak slope $p = 0.0395$), together explaining 56.72% of the variance.

For motor learning of temporal adaptation, we observed a significant positive correlation between increased MEP_{max} after AIH and higher STA during motor learning (Adjusted $R^2 = 0.496$, $p = 0.006$). Furthermore, the correlation between increased area under the recruitment curve after AIH and heightened STA approached significance (Adjusted $R^2 = 0.189$, $p = 0.088$), as did the correlation between increased peak slope post-AIH and more positive STA (Adjusted $R^2 = 0.233$, $p = 0.064$). Utilizing stepwise linear regression, ΔMEP_{max} , Δ area under the recruitment curve, and Δ RMT emerged as the best predictors of changes in STA during motor learning ($\Delta STA = 0.015 + 0.245 * \Delta$

MEP_{max} – 0.071 * Δ area under the recruitment curve + 0.008 * Δ RMT, AIC = -76.15, model p = 0.055, MEP_{max} p = 0.0297, area under the recruitment curve p = 0.120, RMT p = 0.194), explaining 51.82% of the variance. Conversely, none of the TMS indices showed a significant correlation with decreased DSA during motor learning (model p = 0.967). In summary, TMS indices reflecting changes in CSE after AIH significantly predicted the magnitude of motor learning observed for both SLA and STA.

Lower Limb Excitability Predicts Motor Learning: Net Metabolic Power

Interestingly, net metabolic power significantly correlated with Δ MEP_{max} (Adjusted R² = 0.666, p = 0.001), Δ area under the recruitment curve (Adjusted R² = 0.649, p = 0.001), and Δ peak slope (Adjusted R² = 0.313, p = 0.034), while Δ RMT approached significance (Adjusted R² = 0.204, p = 0.079). Stepwise linear regression identified Δ MEP_{max} as the most significant predictor of reduced net metabolic power during motor learning (Δ net metabolic power = 0.161 + 0.875 * Δ MEP_{max}, AIC = -38.35, model p = 0.021). Together, these results suggest that TMS indices of CSE were significant predictors of the decrease in net metabolic power that accompanies spatiotemporal adaptation during motor learning.

Motor Savings: Spatiotemporal Asymmetry

We characterized motor savings by quantifying the magnitude of spatiotemporal adaptation retained during initial Adapt 2 compared to initial Adapt 1 (Fig. 5A-C)²⁴. We observed significant savings of spatial symmetry, as evidenced by more symmetric step lengths during initial Adapt 2 relative to initial Adapt 1 (t(11) = -4.46, p < 0.001) and during late Adapt 2 relative to late Adapt 1 (t(11) = -4.70, p < 0.001). Additionally, we found significant savings of both STA and DSA. STA was significantly higher during initial Adapt 2 compared to initial Adapt 1 (t(11) = -2.35, p = 0.039), as well as from late Adapt 2 compared to late Adapt 1 (t(11) = -2.41, p = 0.035). For DSA, Tukey's post-hoc comparisons identified significantly lower asymmetry during initial Adapt 2 compared to initial Adapt 1 (t(11) = 4.43, p = 0.001) and from late Adapt 2 compared to late Adapt 1 (t(11) = 3.02, p = 0.012). Therefore, participants displayed motor savings of both spatial and temporal parameters of adaptation.

Motor Savings: Net Metabolic Power

We assessed savings of metabolic adaptation by comparing net metabolic power during early Adapt 2 to early Adapt 1 (Fig. 5D). Tukey's pairwise comparisons indicated significantly lower net metabolic power during early Adapt 2 compared to early Adapt 1 ($t(11) = 3.75$, $p = 0.003$), demonstrating that participants retained improved metabolic efficiency. The mean net metabolic power during early Adapt 2 was 5.39 W/kg (SE = 0.33), with a 0.7 W/kg reduction compared to early Adapt 1.

Lower Limb Excitability Predicts Motor Savings: Spatiotemporal Asymmetry

To evaluate how well $\Delta \text{MEP}_{\text{max}}$, Δ area under the recruitment curve, Δ peak slope, and ΔRMT explained the variance in motor savings outcomes, we conducted linear regression analyses and computed adjusted R^2 values (Fig. 6, Table 2).

A significant positive correlation was observed between elevated MEP_{max} following AIH and the savings of lower SLA (Adjusted $R^2 = 0.625$, $p = 0.001$). Furthermore, the increased area under the recruitment curve positively correlated with the savings of lower SLA (Adjusted $R^2 = 0.290$, $p = 0.041$). Stepwise linear regression identified $\Delta \text{MEP}_{\text{max}}$ and Δ peak slope as the two best predictors of SLA savings ($\Delta \text{SLA} = 0.053 + 0.416 * \Delta \text{MEP}_{\text{max}} - 0.366 * \Delta$ peak slope, AIC = -75.05, model $p = 0.005$, MEP_{max} $p = 0.002$, slope $p = 0.0423$), explaining 77.33% of the variance.

Linear regression analyses also revealed a significant positive correlation between increased MEP_{max} after AIH and the savings of elevated STA (Adjusted $R^2 = 0.538$, $p = 0.004$). Additionally, we observed a significant positive correlation between the elevated area under the recruitment curve and the savings of higher STA (Adjusted $R^2 = 0.307$, $p = 0.036$). Stepwise linear regression indicated that both $\Delta \text{MEP}_{\text{max}}$ and Δ peak slope were the primary predictors of STA savings ($\Delta \text{STA} = 0.002 + 0.203 * \Delta \text{MEP}_{\text{max}} - 0.152 * \Delta$ peak slope, AIC = -79.24, model $p = 0.065$, MEP_{max} $p = 0.039$, peak slope $p = 0.261$).

Both the $\Delta \text{MEP}_{\text{max}}$ and Δ peak slope explained 49.03% of the variance in STA savings. However, no significant correlations were observed between any of the TMS indices and the savings of lower DSA (model $p = 0.468$). These results suggest that TMS

indices of CSE were strong predictors of the degree of motor savings observed for both SLA and STA.

Lower Limb Excitability Predicts Motor Savings: Net Metabolic Power

Net metabolic power exhibited a robust positive correlation with Δ MEP_{max} (Adjusted R² = 0.645, p = 0.001), Δ the area under the recruitment curve (Adjusted R² = 0.693, p < 0.001), and Δ peak slope (Adjusted R² = 0.406, p = 0.015), with Δ RMT approaching significance (p = 0.065). Stepwise linear regression analysis identified Δ area under the recruitment curve as the best predictor of net metabolic power savings (Δ net metabolic power = 0.251 + 0.776 * Δ area under the recruitment curve, AIC = -22.76, model p = 0.024). Overall, we found that TMS indices representing changes in CSE post-AIH significantly predicted the savings of lower net metabolic power upon subsequent split-belt walking exposures.

Spatiotemporal Asymmetry Predicts Net Metabolic Power

Both Δ SLA and Δ STA significantly correlated with Δ net metabolic power during motor learning (Δ SLA Adjusted R² = 0.452, p = 0.010; Δ STA Adjusted R² = 0.396, p = 0.017) and motor savings (Δ SLA Adjusted R² = 0.461, p = 0.009; Δ STA Adjusted R² = 0.468, p = 0.008). In contrast, Δ DSA did not correlate with Δ net metabolic power (motor learning p = 0.734; motor savings p = 0.580). While changes in spatiotemporal asymmetry significantly predicted improvements in metabolic efficiency (Supplementary Fig. S1), changes in MEP_{max} and the area under the recruitment curve explained a greater portion of the variance in net metabolic power.

Retrospective Comparison of Learning Between a Mild vs. Large Perturbation

To better understand how perturbation size affects motor learning and motor savings after AIH, we retrospectively compared the degree of spatiotemporal and metabolic adaptation between a large 1:2 belt speed ratio and a milder 1:1.5 belt speed ratio reported in Bogard et al. 2023 (See Supplementary Fig. S2). The results of the statistical tests are summarized in Supplementary Table S3. Briefly, Tukey's post-hoc analyses indicated that the large perturbation group achieved more symmetrical step lengths during both motor learning and motor savings compared to the mild perturbation group. The average

decrease in SLA for the large perturbation group was 0.09 lower during motor learning (SE = 0.03) and 0.07 lower during motor savings (SE = 0.03) than the mild perturbation group. The large perturbation group also demonstrated greater motor savings of STA, maintaining an average STA that was 0.04 higher than the mild perturbation group (SE = 0.02). Both the mild and large perturbation groups displayed similar magnitudes of motor learning and motor savings of DSA. The large perturbation group exhibited greater savings of improved metabolic efficiency, with net metabolic power that was an average of 0.57 W/kg lower than the mild perturbation group (SE = 0.20). Although we did not find a significant group difference in net metabolic power during motor learning, the large perturbation group averaged 0.35 W/kg lower than the mild perturbation group (SE = 0.20). Overall, the larger perturbation led to greater motor learning of SLA and more prominent motor savings of SLA, STA, and metabolic efficiency.

Discussion

Our results provide the first evidence that repetitive AIH amplifies excitability to the lower limb, supporting our primary hypothesis. Significantly, this enhanced excitability post-AIH is associated with both improved motor learning and motor savings, confirming our secondary hypothesis. Furthermore, our study demonstrates a novel association between elevated lower limb excitability and greater metabolic efficiency. Together, these results indicate that both changes in excitability and reductions in net metabolic power are markers of AIH-mediated neuroplasticity.

AIH Increases Lower Limb Excitability

Our results advance the understanding of AIH-induced neuroplasticity beyond the upper limb by demonstrating that repetitive AIH increases TA MEP_{max}, area under the recruitment curve, and MEP amplitudes at both 120% and 140% of RMT. Additionally, our study did not detect any concurrent changes in the maximal voluntary contraction after AIH, aligning with prior research²⁶. This suggests that changes in maximal voluntary contraction may not parallel changes in descending and spinal excitability in able-bodied individuals. While the composite nature of MEPs precludes the differentiation of the specific contributions of intracortical and transcortical networks to behavioral outcomes²⁷,

our collective findings indicate that AIH increases net motoneuronal excitability. Indeed, prior research on the upper limb has shown increases in both CSE and spike-timing-dependent plasticity after a single AIH dose, whereas measures of intracortical inhibition and facilitation remained unchanged⁹. Although we did not examine spinal excitability, Finn et al. (2022) observed a lower threshold for eliciting the soleus H-reflex after AIH, indicating enhanced efficacy of the Ia-afferent-motoneuronal pathway. Together with our observations suggest that AIH enhances motoneuronal excitability.

It is important to acknowledge that inconsistent findings have been reported. Discrepancies may be partially attributed to variations in AIH dosing. For instance, compared to Christiansen et al. (2018) and our study, Finn et al. (2022) only observed increased CSE at discrete time points while utilizing a more conservative desaturation threshold of 75% and omitting the remaining hypoxic interval. In contrast, Radia et al. (2022) implemented a longer 3-minute hypoxic interval and did not detect changes in CSE. Notably, we observed significant increases in CSE with multiple-day AIH administration, utilizing dosing intervals that conferred improvements in walking performance after iSCI^{2,3}. Given the distinct cortical representations²⁸ and varying motor thresholds of upper and lower limb muscles²⁹, it is also plausible that AIH may not produce the same magnitude of change across all motoneuron pools. Nevertheless, our findings of increased TA excitation after repetitive AIH suggest potential applications in neurorehabilitation to promote adaptive neuroplasticity.

Lower Limb Excitability Predicts Motor Learning and Motor Savings

To our knowledge, this is the first study to examine the functional significance of AIH-induced enhancements in CSE in humans. We demonstrate that the degree of CSE enhancement post-AIH predicts gains in motor learning, as evidenced by a positive correlation between increased MEP_{max} and greater spatiotemporal adaptation. Additionally, increased MEP_{max} and area under the recruitment curve post-AIH both correlate with larger savings of spatiotemporal adaptation. We argue for the interpretation that enhanced CSE is not only a marker of AIH-mediated neuroplasticity but also supports the processes that underlie the acquisition and savings of new motor skills. This is

supported by preceding investigations that have linked CSE to improvements in both motor learning^{30,31} and motor savings^{15,32}.

The argument can be made that if heightened CSE supports motor learning processes, individuals who do not exhibit an increase in CSE after AIH may not learn the task. However, able-bodied individuals can still acquire new motor skills without changes^{22,24} or even with decreases in CSE³³. Indeed, participants with no changes or decreases in CSE still successfully adapted spatiotemporal coordination, albeit to a lesser extent (Fig. 5). It is also possible that increased motor learning after AIH¹² further drives increases in CSE. However, it is unlikely that improvements in motor learning alone facilitate increases in CSE as motor training paradigms show that elevated CSE only persists with additional task challenges^{17,34}. Moreover, we distinctively evaluated changes in CSE before assessing motor learning within a conservative 75-minute window. While we did not assess longitudinal changes in CSE, previous research indicates CSE remains elevated for up to 75 minutes after a single AIH dose⁹. Therefore, our results suggest that even transient increases in CSE after repetitive AIH predict improvements in both motor learning and motor savings.

Of particular interest is that we characterized improvements in motor learning and motor savings without any concurrent motor training paradigm. Previous work in humans demonstrated that AIH paired with task-specific motor training further amplifies walking performance after iSCI compared to AIH or training alone^{2,3}. Motor training may further potentiate changes in AIH-induced neuroplasticity as longitudinal human studies have shown that progressively challenging motor training enhances both motor learning and CSE^{17,35}.

Enhanced Excitability Predicts Greater Reductions in Net Metabolic Power

Our findings reveal an unprecedented positive correlation between increased CSE and improved metabolic efficiency for both motor learning and motor savings. Specifically, increased MEP_{max}, area under the recruitment curve, and peak slope all positively correlate with reduced net metabolic power. Therefore, improved metabolic efficiency could serve as a marker of AIH-induced neuroplasticity. This interpretation is supported by our previous study, where the AIH group displayed lower net metabolic power at the

start of the novel task and uniquely demonstrated significant savings of improved metabolic efficiency¹².

Considering that improved metabolic efficiency is a feature of gains in motor learning³⁶, it is plausible that the reductions in net metabolic power are primarily driven by improvements in spatiotemporal adaption. However, we observed that most of the TMS indices explained more variance in net metabolic power than spatiotemporal asymmetry. This indicates that metabolic efficiency cannot be explained by changes in biomechanics alone and that net metabolic power provides an additional marker of AIH-mediated neuroplasticity.

Potential Mechanisms of Increased CSE

Evidence from rodent models suggests that BDNF-dependent mechanisms play a central role in AIH-mediated neuroplasticity^{4–6}. Therefore, it is plausible that BDNF may serve as the intermediary link between AIH-induced increments in CSE and enhancements in motor learning. Prior investigations in exercise-dependent increases in BDNF³⁷ substantiate this interpretation by showing concomitant increases in CSE and motor learning¹⁴. Conversely, individuals with a BDNF val66met polymorphism, known to decrease activity-dependent BDNF secretion, do not exhibit a significant change in CSE following a complex motor task³⁸, whereas increasing CSE through motor cortex stimulation enhances motor learning¹³.

While our study did not assess the involvement of BDNF, its established role in contributing to energy efficiency³⁹ by promoting synaptic plasticity⁴⁰ and corticospinal synaptogenesis⁴¹ could suggest that heightened CSE after AIH may facilitate BDNF-mediated energy efficiency. Critical for this interpretation, the AIH-dependent upregulation of BDNF has been shown to strengthen excitatory glutamatergic synapses in rodents with iSCI⁴². Importantly, rodents with increased BDNF signaling demonstrate increased excitatory neurotransmission and plasticity⁴³. In humans, genetic disruption of BDNF impairs the formation of excitatory glutamatergic synapses⁴⁴. Future studies are needed to clarify the role of BDNF in regulating metabolic efficiency in humans.

Larger Perturbations May Promote Better Motor Savings

While our previous study revealed significant improvements in motor learning and savings after AIH at a mild perturbation¹², it remains unclear whether AIH-induced enhancements in CSE differentially facilitate motor learning and savings with higher levels of difficulty. Prior work found that continuously increasing the task difficulty drives persistent increases in CSE¹⁷. Additionally, earlier studies have demonstrated that greater challenges, such as larger split-belt speed perturbations, result in enhanced motor learning and savings²⁴. Consistent with earlier findings²⁴, we observed greater motor learning and savings of SLA with the large perturbation. Notably, we also observed greater savings of higher STA and improved metabolic efficiency with the large perturbation. Our findings suggest that AIH-induced increases in CSE may exert distinct effects as the challenge increases, with greater challenges leading to more substantial enhancements in both motor learning and metabolic efficiency. Tailoring task difficulty has the potential to optimize rehabilitation strategies post-AIH.

In conclusion, our study not only uncovers the positive effects of repetitive AIH on lower limb excitability, but also establishes its critical role in predicting motor learning, motor savings, and metabolic efficiency. Optimizing motor learning to drive gains in motor function after neurological injury necessitates a closer examination of the interplay between AIH-induced corticospinal plasticity and the structure of motor training during rehabilitation.

Methods

Participants

Thirteen able-bodied subjects between the ages of 18 to 65 participated in the study at the University of Colorado, Boulder (Females = 7; Mean age = 23.4 ± 1.8 years; Mean height = 173.6 ± 9.4 cm; Mean weight = 72.6 ± 17.0 kg). Demographic characteristics are summarized in Supplementary Table S4. An a priori analysis determined that a sample size of 12 participants would be sufficient to detect significant difference in corticospinal excitability (CSE) across 2 time points (e.g., pre-AIH and post-AIH) with >80% power. Exclusion criteria comprised a history of cardiovascular disease, pulmonary complications, pain, syncope, sensitivity to altitude, or currently pregnant or undergoing physical therapy. All participants provided written informed consent from the Colorado

Multiple Institutional Review Board (COMIRB #20-0689) before participation. The study adhered to the principles of the Declaration of Helsinki, and registration was completed at clinicaltrials.gov (NCT05341466; 22/04/2022).

Experimental Design

Subjects visited the laboratory for five consecutive days to participate in experiments. On the first day, we assessed baseline TA excitability using TMS before administering the first dose of AIH ('pre-TMS'). Following the pre-TMS session, all thirteen participants received AIH for five consecutive days at the same time each day. Participants were not informed of whether they received AIH or normoxic air. Prior evidence indicates that participants cannot distinguish between AIH vs. SHAM exposures (i.e., normoxic air)⁴⁵. A single AIH dose entailed 15 cycles, each comprised of 90-second intervals of breathing low-oxygen air ($9\% \pm 2\% \text{ O}_2$) alternated with 60-second intervals of breathing ambient air ($21\% \pm 2\% \text{ O}_2$)³. During AIH, two trained operators manually regulated the supply of low-oxygen air by connecting a hose to a non-rebreather mask⁴⁶. We recorded oxygen saturation (SpO_2) and heart rate (HR) at 1 Hz while blood pressure (BP) was measured every five cycles (Masimo; Irvine, CA). We paused the hypoxic interval if SpO_2 fell below 70%, HR exceeded 160 bpm or systolic BP went above 160 mmHg and resumed once SpO_2 returned above 80%, HR dropped below 140 bpm, and systolic BP decreased below 140 mmHg. The experiment terminated if the participant reported pain, dizziness, diaphoresis, tinnitus, or blurred vision. On the last day, participants underwent a second TMS session within 15 minutes after completing their final dose of AIH ('post-TMS'). The split-belt walking task was performed following the second TMS session to ensure that motor learning did not influence CSE.

Transcranial Magnetic Stimulation Protocol

To examine alterations in resting CSE, we utilized monophasic, single-pulse TMS (DuoMAG MP-Dual Magnetic Stimulator; Deymed, Czechia) to target the leg motor area of the primary motor cortex⁴⁷. We positioned an insulated, double-cone coil (DuoMAG Butterfly V-Shaped Coil; Magstim, UK) 0-2 cm posterior to the vertex to evoke MEPs in the TA muscle, targeting the region that obtained the lowest threshold and shortest

latency response⁴⁸ recorded via surface electromyography (EMG) (Bipolar Ag/AgCl, spaced 22mm apart, Noraxon Inc., USA). Notably, resting TA MEPs are highly reproducible⁴⁹ and the TA requires a lower stimulus intensity than other muscles⁵⁰. Prior studies have established a close link between corticospinal drive and TA excitability⁵¹. Additionally, enhancing TA excitability holds clinical significance as it would improve foot clearance during walking after iSCI⁵².

We utilized a generic brain MRI scaled to anatomical references and an NDI Polaris Vicra camera for real-time navigation of the TMS coil (Visor2, ANT-NeuroNav, Netherlands). The hotspot was defined as the stimulation vector that elicited 4 MEPs \geq 50 μ V out of 7 trials⁵³. The resting motor threshold (RMT) was determined as the lowest stimulus intensity to elicit at least 4/7 MEPs \geq 50 μ V over the hotspot. We used 7 trials as a conservative intermediary between the commonly used 5-trial criterion⁵⁴ and the 10-trial criterion⁵⁵.

Recruitment curves were generated by plotting the peak-to-peak amplitudes of the TA MEPs against their corresponding stimulus intensities. To compare changes in CSE across participants and testing sessions pre- to post-AIH, we normalized the recruitment curves to the RMT during each respective testing session¹¹. Thus, the recruitment curve sampling involved a pseudo-randomized sequence of stimulations ranging from 90% to 140% of the RMT^{56,57}, with 6 pulses applied per intensity (Signal; CED, USA)⁵⁸. We delivered TMS stimuli in 15-second intervals with a 15% time variation to prevent synaptic fatigue and minimize MEP variability⁵⁹.

Split-Belt Walking Protocol

During the split-belt walking protocol, participants learned to walk on treadmill belts set at different speeds (D-flow v3.34.3; Motek, Netherlands). We secured participants into a passive safety harness and instructed them to refrain from using the handrails. To prevent inadvertent stepping onto the contralateral treadmill belt, participants were permitted to observe their feet in a mirror¹².

The split-belt walking protocol comprised of four walking conditions: (1) 'Baseline', with matched belt speeds set at 1 m/s for 300 strides, (2) 'Adapt 1', involving a 2:1 split-belt speed ratio for 300 strides, (3) 'Washout', with tied-belts set at 1 m/s for 350 strides,

and (4) 'Adapt 2', replicating the 2:1 split-belt speed ratio for 300 strides²⁴. The perturbed belt was randomized⁶⁰. Importantly, participants remained unaware that the leg perturbed during the split-belt walking protocol corresponded to the same leg used for recording surface EMG during the TMS protocol. We increased the belt speed 15-30 strides into the adaptation condition to blind the subjects to the timing¹².

Data Collection

Electromyography. We placed bipolar Ag/AgCl electrodes, spaced 22 mm apart, over the TA, one-third of the distance from the fibular head to the lateral malleolus, and a ground electrode over the patella (Noraxon Inc., USA)⁶¹. To obtain low impedance (< 5 kΩ), we first shaved and cleaned the skin with an isopropyl alcohol wipe⁶². EMG signals were bandpass filtered within a range of 20-1000 Hz, amplified by a gain 100 (CED 1902), sampled at 10 kHz (CED 1401), and displayed in real-time using Signal software (CED, USA).

Maximal voluntary contraction. Before the first AIH dose and after the fifth and final AIH dose, participants were instructed to generate three, 5-second maximal dorsiflexion contractions against a resistive load, with a minimum 1-minute rest between trials⁶³. We directed participants to contract their TA as forcefully and rapidly as possible without engaging their thigh muscles⁶⁴. If the maximal peak-to-peak amplitude varied by more than 10%, the participant performed additional contractions⁶⁵. We defined the maximal voluntary contraction as the highest value obtained.

Kinematics. A 10-camera motion system captured lower limb kinematic data at a sampling frequency of 100 Hz (Vicon Nexus v2.8.1; Vicon Motion Systems, UK). We bilaterally placed reflective markers over the shank and thigh, as well as on the anterior and posterior superior iliac spines, iliac crests, greater trochanters, medial and lateral femoral epicondyles, medial and lateral malleoli, calcanei, and first and fifth metatarsal heads¹². We analyzed kinematic data using custom pipelines in Visual3D (v2021.11.3; C-motion Inc., MD) and MATLAB (R2023b; MathWorks, Inc., US).

Kinetics. Three-dimensional ground reaction forces (GRF) were collected at a sampling frequency of 1,000 Hz (D-flow v3.34.3; Motek, Netherlands) and low-pass filtered with a fourth-order Butterworth filter at a cutoff frequency of 20 Hz⁶⁶. We used GRFs to validate gait events.

Expired gas analysis. We measured the rate of oxygen consumption (VO_2) and carbon dioxide production (VCO_2) using open circuit spirometry (TrueOne 2400; ParvoMedics Inc., UT). Resting metabolic rate was estimated based on the average VO_2 and VCO_2 of the last 2 minutes of a 5-minute standing trial and was subtracted from the subsequent net metabolic power measured during walking²². The mean resting metabolic rate was 1.42 W/kg (SE = 0.05). Respiratory exchange ratios (RER; VCO_2/VO_2) below 1 indicated predominant utilization of aerobic pathways⁶⁷.

Data Analysis

Maximum Motor Evoked Potential. The MEP onset was identified using custom configurations in Signal (CED, USA) as the first frame at which the peak-to-peak amplitude exceeded three standard deviations of the background EMG⁴⁹ recorded 200 ms preceding the TMS stimuli²³. To account for the pre-stimulus baseline TA activation, we subtracted the mean background EMG from all MEPs⁶⁸. We averaged the peak-to-peak MEP amplitudes across all thirteen participants and quantified the change in MEP_{max} pre-AIH and post-AIH ($\Delta \text{MEP}_{\text{max}}$).

Area Under the Recruitment Curve. We calculated the area under the recruitment curve both pre- and post-AIH (Δ area under the recruitment curve) using the trapezoidal method of area estimation. The area under the recruitment curve provides a crude measure of overall net excitability from 90% to 140% of RMT⁶⁹.

Recruitment Curve Slope. The recruitment curve slope was determined by fitting a Boltzmann distribution in MATLAB using the Levenberg-Marquardt algorithm, as shown in Equation 1⁷⁰. The Boltzmann equation is a function of stimulus intensity (s) and response amplitude (MEP), where MEP_{max} is the maximum averaged response from the

recruitment curve, s_{50} is the stimulus intensity required to produce a response with half the amplitude of MEP_{max} , and k is the slope parameter⁷¹.

$$MEP(s) = \frac{MEP_{max}}{1 + e^{(s_{50}-s)/k}} \text{ (Equation 1)}$$

Peak slope, the inverse of the slope parameter, represents the rate of the MEP increase relative to MEP_{max} and is used to quantify the change in the gain of excitability⁵⁸. We calculated alterations in peak slope pre-AIH and post-AIH (Δ peak slope).

Resting Motor Threshold. RMT represents the motor threshold required to excite the TA at rest⁵³. We compared the RMT before and after AIH (Δ RMT).

Spatiotemporal Asymmetry. We identified heel-strike and toe-off gait events for each stride using a vertical GRF detection threshold of 30 N⁷². These gait events were utilized to calculate step length asymmetry (SLA), step time asymmetry (STA), and double support time asymmetry (DSA). Step lengths and step times were determined by the fore-aft contralateral calcanei markers at heel-strike, while double support times were defined as the duration between the leading limb's heel-strike and contralateral toe-off⁷³. We computed asymmetry values using Equation 2⁷⁴, where values of 0 indicate perfect symmetry.

$$\text{Asymmetry} = \frac{\text{Fast leg} - \text{Slow leg}}{\text{Fast leg} + \text{Slow leg}} \text{ (Equation 2)}$$

The phases 'initial learning' and 'late learning' were defined as the first five strides after the speed perturbation and the final twenty strides, respectively²⁴. We assessed motor learning by examining the magnitude of spatiotemporal adaptation from initial Adapt 1 to late Adapt 1 and motor savings by the extent of adaptation from initial Adapt 1 to initial Adapt 2. Enhanced motor learning and motor savings were characterized by reductions in SLA and DSA towards symmetry values of 0, coupled with augmentations in STA towards positive asymmetry. This is supported by extensive research demonstrating these adaptation patterns in able-bodied individuals^{25,75,76}. Given evidence of a distinct mode-dependency in the neural control of split-belt walking compared to split-belt running⁷⁷, we excluded one participant from gait analyses due to utilizing a running strategy with a distinct aerial phase during both Adapt 1 and Adapt 2.

Net Metabolic Power. We quantified metabolic power using a standard regression equation⁷⁸. The mean resting metabolic rate was subtracted from metabolic power and then normalized to body mass to compute net metabolic power (W/kg)⁷⁹. We omitted the first minute of each condition to account for the time lag of the expired gas reaching the mixing chamber¹². Thus, we defined ‘early’ and ‘late’ net metabolic power as the second and last minute of each condition, respectively²². We characterized the extent of metabolic adaptation during motor learning by assessing the difference in net metabolic power from early Adapt 1 to late Adapt 1. Additionally, we characterized metabolic savings by comparing early Adapt 1 and early Adapt 2.

Retrospective Comparisons. To gain deeper insights into how perturbation size affects AIH-induced enhancements in motor learning and motor savings, we conducted a retrospective analysis comparing the magnitude of spatiotemporal and metabolic adaptation between a large 1:2 belt speed ratio and a milder 1:1.5 belt speed ratio. The mild perturbation group comprised a subset of participants from the AIH group reported in Bogard et al. (2023). Converging evidence suggests that increasing task difficulty can improve subsequent motor learning^{24,35} and potentiate cortical plasticity¹⁷. Thus, the primary objective of this analysis was to determine whether AIH further enhances motor learning and motor savings under greater challenges, considering its demonstrated efficacy even under mild challenges¹². Determining specific split-belt walking parameters that optimize motor learning and motor savings will clarify our understanding of the effects of AIH on locomotor adaptation.

Statistical Analysis

Statistical analyses of the experimental data were conducted in R Studio (v2021.09.0) with a significance level set at $p < 0.05$. Group data are presented as mean \pm standard error (SE). We evaluated normality using the Shapiro-Wilks test, multicollinearity using the variance of inflation factor, and sphericity using Mauchly’s Test.

Background EMG. To evaluate the consistency of the pre-stimulus background EMG between pre-AIH and post-AIH TMS sessions, we conducted a paired t-test.

TA excitability. We assessed alterations in TA excitability pre-AIH and post-AIH using paired t-tests for normally distributed data and Wilcoxon signed-rank tests when normality assumptions were not met. Specifically, we used paired t-tests to analyze changes in the maximal voluntary contraction, and Wilcoxon signed-rank tests to assess changes in MEP_{max}, area under the recruitment curve, peak slope, and RMT. In addition, we conducted a repeated measures ANOVA with the Greenhouse-Geisser degrees of freedom correction to compare the peak-to-peak MEP amplitude pre-AIH and post-AIH at the stimulus intensities of 100% RMT, 120% RMT, and 140% RMT, with the within-factors of 'stimulus intensity' (100%, 120%, and 140% RMT) and 'timepoint' (pre-AIH and post-AIH). We conducted post hoc analyses utilizing Tukey's honest significant difference method to correct for multiple comparisons.

Adaptation. We conducted a two-way ANOVA to investigate the main effects of the within-factors 'condition' and 'learning phase' on spatiotemporal asymmetry (SLA, STA, DSA) and net metabolic power. We treated the subject identification number as a random factor to acknowledge that the same participants were measured across different levels of the within-subject factors, contributing to a repeated measures design. Assumptions of sphericity were not violated for any of the dependent variables; thus, corrections were not applied. Subsequently, we conducted two Tukey's post-hoc tests for each ANOVA to explore any potential significant pairwise comparisons. We used Tukey's pairwise comparisons to analyze motor learning of spatiotemporal symmetry between initial Adapt 1-late Adapt 1 and initial Adapt 2-late Adapt 2. Additionally, comparisons were made between early Adapt 1-late Adapt 1 to evaluate metabolic adaptation. We also performed Tukey's pairwise comparisons between initial Adapt 1-initial Adapt 2 and late Adapt 1-late Adapt 2 to assess savings of spatiotemporal adaptation, as well as between early Adapt 1-early Adapt 2 to examine savings of metabolic efficiency.

Correlations. We performed linear regression analyses between TMS indices of CSE and motor learning outcomes, as well as between TMS indices of CSE and motor savings outcomes. To compare how well TMS indices of CSE explained the variance in net metabolic power compared to parameters of spatiotemporal asymmetry, we also performed linear regression analyses with Δ SLA, Δ STA, and Δ DSA as the predictors and Δ net metabolic power as the outcome variable. We calculated the adjusted R^2 values for each linear regression to measure the proportion of the variance in behavior explained by changes in CSE. In addition, we used stepwise linear regression models to iteratively eliminate insignificant predictor variables. For each model, the predictor variables were Δ MEP_{max}, Δ area under the recruitment curve, Δ peak slope, and Δ RMT, and the dependent variables were the motor learning and motor savings outcomes (Δ SLA, Δ STA, Δ DSA, and Δ net metabolic power). The final stepwise linear regression model was determined based on achieving the lowest Akaike information criterion (AIC) and highest adjusted R^2 value.

Retrospective comparisons. We compared motor learning and motor savings between a mild and a large perturbation. To address differences in sample size, we utilized linear mixed models, incorporating Satterthwaite's method for estimating degrees of freedom. Subsequently, we used an ANOVA to assess significance, with perturbation size as the between-group factor (1:1.5 belt speed ratio and 1:2 belt speed ratio) and adaptation period as the within-group factor (Δ motor learning and Δ motor savings). Significant ANOVAs were followed by Tukey's post-hoc analysis to adjust for multiple comparisons.

References

1. Trumbower, R. D., Jayaraman, A., Mitchell, G. S. & Rymer, W. Z. Exposure to Acute Intermittent Hypoxia Augments Somatic Motor Function in Humans With Incomplete Spinal Cord Injury. *Neurorehabil Neural Repair* **26**, 163–172 (2012).
2. Hayes, H. B. *et al.* Daily intermittent hypoxia enhances walking after chronic spinal cord injury: A randomized trial. *Neurology* **82**, 104–113 (2014).
3. Tan, A. Q., Sohn, W. J., Naidu, A. & Trumbower, R. D. Daily acute intermittent hypoxia combined with walking practice enhances walking performance but not intralimb motor coordination in persons with chronic incomplete spinal cord injury. *Experimental Neurology* **340**, 113669 (2021).
4. Baker-Herman, T. L. *et al.* BDNF is necessary and sufficient for spinal respiratory plasticity following intermittent hypoxia. *Nat Neurosci* **7**, 48–55 (2004).
5. Satriotomo, I. *et al.* Repetitive acute intermittent hypoxia increases growth/neurotrophic factor expression in non-respiratory motor neurons. *Neuroscience* **322**, 479–488 (2016).

6. Lovett-Barr, M. R. *et al.* Repetitive Intermittent Hypoxia Induces Respiratory and Somatic Motor Recovery after Chronic Cervical Spinal Injury. *Journal of Neuroscience* **32**, 3591–3600 (2012).
7. Navarrete-Opazo, A., Alcayaga, J., Sepúlveda, O., Rojas, E. & Astudillo, C. Repetitive Intermittent Hypoxia and Locomotor Training Enhances Walking Function in Incomplete Spinal Cord Injury Subjects: A Randomized, Triple-Blind, Placebo-Controlled Clinical Trial. *Journal of Neurotrauma* **34**, 1803–1812 (2017).
8. Spampinato, D. A., Ibanez, J., Rocchi, L. & Rothwell, J. Motor potentials evoked by transcranial magnetic stimulation: interpreting a simple measure of a complex system. *The Journal of Physiology* **601**, 2827–2851 (2023).
9. Christiansen, L., Urbin, M., Mitchell, G. S. & Perez, M. A. Acute intermittent hypoxia enhances corticospinal synaptic plasticity in humans. *eLife* **7**, e34304 (2018).
10. Finn, H. T. *et al.* The effect of acute intermittent hypoxia on human limb motoneurone output. *Experimental Physiology* **107**, 615–630 (2022).
11. Radia, S. *et al.* Effects of acute intermittent hypoxia on corticospinal excitability within the primary motor cortex. *Eur J Appl Physiol* **122**, 2111–2123 (2022).
12. Bogard, A. T., Hemmerle, M. R., Smith, A. C. & Tan, A. Q. Enhanced motor learning and motor savings after acute intermittent hypoxia are associated with a reduction in metabolic cost. *The Journal of Physiology* JP285425 (2023) doi:10.1113/JP285425.
13. Fritsch, B. *et al.* Direct Current Stimulation Promotes BDNF-Dependent Synaptic Plasticity: Potential Implications for Motor Learning. *Neuron* **66**, 198–204 (2010).
14. Mang, C. S., Snow, N. J., Campbell, K. L., Ross, C. J. D. & Boyd, L. A. A single bout of high-intensity aerobic exercise facilitates response to paired associative stimulation and promotes sequence-specific implicit motor learning. *Journal of Applied Physiology* **117**, 1325–1336 (2014).
15. Hirano, M., Kubota, S., Tanabe, S., Koizume, Y. & Funase, K. Interactions Among Learning Stage, Retention, and Primary Motor Cortex Excitability in Motor Skill Learning. *Brain Stimulation* **8**, 1195–1204 (2015).
16. Sarwary, A. M. E., Wischnewski, M., Schutter, D. J. L. G., Selen, L. P. J. & Medendorp, W. P. Corticospinal correlates of fast and slow adaptive processes in motor learning. *Journal of Neurophysiology* **120**, 2011–2019 (2018).
17. Christiansen, L. *et al.* Long-term motor skill training with individually adjusted progressive difficulty enhances learning and promotes corticospinal plasticity. *Sci Rep* **10**, 15588 (2020).
18. Bagce, H. F., Saleh, S., Adamovich, S. V., Krakauer, J. W. & Tunik, E. Corticospinal excitability is enhanced after visuomotor adaptation and depends on learning rather than performance or error. *Journal of Neurophysiology* **109**, 1097–1106 (2013).
19. Perez, M. A., Lungholt, B. K. S., Nyborg, K. & Nielsen, J. B. Motor skill training induces changes in the excitability of the leg cortical area in healthy humans. *Exp Brain Res* **159**, 197–205 (2004).
20. Dambreville, C., Neige, C., Mercier, C., Blanchette, A. K. & Bouyer, L. J. Corticospinal Excitability Quantification During a Visually-Guided Precision Walking Task in Humans: Potential for Neurorehabilitation. *Neurorehabil Neural Repair* **36**, 689–700 (2022).
21. Cantarero, G., Lloyd, A. & Celnik, P. Reversal of Long-Term Potentiation-Like Plasticity Processes after Motor Learning Disrupts Skill Retention. *Journal of Neuroscience* **33**, 12862–12869 (2013).
22. Finley, J. M., Bastian, A. J. & Gottschall, J. S. Learning to be economical: the energy cost of walking tracks motor adaptation: Split-belt adaptation reduces metabolic power. *The Journal of Physiology* **591**, 1081–1095 (2013).
23. Vargas, C. D. The Influence of Hand Posture on Corticospinal Excitability during Motor Imagery: A Transcranial Magnetic Stimulation Study. *Cerebral Cortex* **14**, 1200–1206 (2004).
24. Leech, K. A., Roemmich, R. T. & Bastian, A. J. Creating flexible motor memories in human walking. *Sci Rep* **8**, 94 (2018).

25. Buurke, T. J. W., Lamothe, C. J. C., Vervoort, D., Van Der Woude, L. H. V. & Den Otter, R. Adaptive control of dynamic balance in human gait on a split-belt treadmill. *Journal of Experimental Biology* jeb.174896 (2018) doi:10.1242/jeb.174896.
26. Tan, A. Q., Tuthill, C., Corsten, A. N., Barth, S. & Trumbower, R. D. A single sequence of intermittent hypoxia does not alter stretch reflex excitability in able-bodied individuals. *Experimental Physiology* EP091531 (2024) doi:10.1113/EP091531.
27. Carson, R. G., Ruddy, K. L. & McNickle, E. What Do TMS-Evoked Motor Potentials Tell Us About Motor Learning? in *Progress in Motor Control* (eds. Laczkó, J. & Latash, M. L.) vol. 957 143–157 (Springer International Publishing, Cham, 2016).
28. Proessl, F. *et al.* Mapping the homunculus: agreement between fMRI and TMS-based motor cortex hand, trunk and leg representations. *Brain Stimulation* **14**, 1692–1693 (2021).
29. De Luca, C. J. & Hostage, E. C. Relationship Between Firing Rate and Recruitment Threshold of Motoneurons in Voluntary Isometric Contractions. *Journal of Neurophysiology* **104**, 1034–1046 (2010).
30. Miyaguchi, S. *et al.* Time course of bilateral corticospinal tract excitability in the motor-learning process. *Neuroscience Letters* **711**, 134410 (2019).
31. Mooney, R. A., Cirillo, J. & Byblow, W. D. Neurophysiological mechanisms underlying motor skill learning in young and older adults. *Exp Brain Res* **237**, 2331–2344 (2019).
32. Centeno, C. *et al.* The effects of aging on cortico-spinal excitability and motor memory consolidation. *Neurobiology of Aging* **70**, 254–264 (2018).
33. Holland, L., Murphy, B., Passmore, S. & Yilder, P. Time course of corticospinal excitability changes following a novel motor training task. *Neuroscience Letters* **591**, 81–85 (2015).
34. Jensen, J. L., Marstrand, P. C. D. & Nielsen, J. B. Motor skill training and strength training are associated with different plastic changes in the central nervous system. *Journal of Applied Physiology* **99**, 1558–1568 (2005).
35. Christiansen, L. *et al.* Progressive practice promotes motor learning and repeated transient increases in corticospinal excitability across multiple days. *Brain Stimulation* **11**, 346–357 (2018).
36. Sánchez, N., Simha, S. N., Donelan, J. M. & Finley, J. M. Using asymmetry to your advantage: learning to acquire and accept external assistance during prolonged split-belt walking. *Journal of Neurophysiology* **125**, 344–357 (2021).
37. Skriver, K. *et al.* Acute exercise improves motor memory: Exploring potential biomarkers. *Neurobiology of Learning and Memory* **116**, 46–58 (2014).
38. Cirillo, J., Hughes, J., Ridding, M., Thomas, P. Q. & Semmler, J. G. Differential modulation of motor cortex excitability in *BDNF* Met allele carriers following experimentally induced and use-dependent plasticity. *Eur J of Neuroscience* **36**, 2640–2649 (2012).
39. Kowiański, P. *et al.* BDNF: A Key Factor with Multipotent Impact on Brain Signaling and Synaptic Plasticity. *Cell Mol Neurobiol* **38**, 579–593 (2018).
40. Mizui, T., Tanimoto, Y., Komatsu, H., Kumanogoh, H. & Kojima, M. The Biological Actions and Mechanisms of Brain-Derived Neurotrophic Factor in Healthy and Disordered Brains. *NM* **05**, 183–195 (2014).
41. Sasaki, M. *et al.* BDNF-Hypersecreting Human Mesenchymal Stem Cells Promote Functional Recovery, Axonal Sprouting, and Protection of Corticospinal Neurons after Spinal Cord Injury. *J. Neurosci.* **29**, 14932–14941 (2009).
42. Golder, F. J. & Mitchell, G. S. Spinal Synaptic Enhancement with Acute Intermittent Hypoxia Improves Respiratory Function after Chronic Cervical Spinal Cord Injury. *J. Neurosci.* **25**, 2925–2932 (2005).
43. Ameroso, D. *et al.* Astrocytic BDNF signaling within the ventromedial hypothalamus regulates energy homeostasis. *Nat Metab* **4**, 627–643 (2022).
44. Sonoyama, T. *et al.* Human BDNF/TrkB variants impair hippocampal synaptogenesis and associate with neurobehavioural abnormalities. *Sci Rep* **10**, 9028 (2020).

45. Barth, S., Slocum, C., Zafonte, R., Tan, A. & Trumbower, R. Blinding Integrity Analysis of a Randomized Clinical Trial to Test the Effects of Therapeutic Intermittent Hypoxia in Able-bodied Adults [Abstract]. *AAPM&R Annual Assembly* (2021).
46. Tan, A. Q., Papadopoulos, J. M., Corsten, A. N. & Trumbower, R. D. An automated pressure-swing absorption system to administer low oxygen therapy for persons with spinal cord injury. *Experimental Neurology* **333**, 113408 (2020).
47. Eisner-Janowicz, I., Chen, B., Sangari, S. & Perez, M. A. Corticospinal excitability across lower limb muscles in humans. *Journal of Neurophysiology* **130**, 788–797 (2023).
48. Kesar, T. M., Stinear, J. W. & Wolf, S. L. The use of transcranial magnetic stimulation to evaluate cortical excitability of lower limb musculature: Challenges and opportunities. *RNN* **36**, 333–348 (2018).
49. Lewis, G. N., Signal, N. & Taylor, D. Reliability of lower limb motor evoked potentials in stroke and healthy populations: How many responses are needed? *Clinical Neurophysiology* **125**, 748–754 (2014).
50. Nielsen, J. B., Pyndt, H. S. & Petersen, N. T. Investigating human motor control by transcranial magnetic stimulation. *Experimental Brain Research* **152**, 1–16 (2003).
51. Capaday, C., Lavoie, B. A., Barbeau, H., Schneider, C. & Bonnard, M. Studies on the Corticospinal Control of Human Walking. I. Responses to Focal Transcranial Magnetic Stimulation of the Motor Cortex. *Journal of Neurophysiology* **81**, 129–139 (1999).
52. Barthélemy, D. *et al.* Impaired Transmission in the Corticospinal Tract and Gait Disability in Spinal Cord Injured Persons. *Journal of Neurophysiology* **104**, 1167–1176 (2010).
53. Nardone, R. *et al.* Assessment of corticospinal excitability after traumatic spinal cord injury using MEP recruitment curves: a preliminary TMS study. *Spinal Cord* **53**, 534–538 (2015).
54. Fujiyama, H., Garry, M. I., Levin, O., Swinnen, S. P. & Summers, J. J. Age-related differences in inhibitory processes during interlimb coordination. *Brain Research* **1262**, 38–47 (2009).
55. Greenhouse, I., King, M., Noah, S., Maddock, R. J. & Ivry, R. B. Individual Differences in Resting Corticospinal Excitability Are Correlated with Reaction Time and GABA Content in Motor Cortex. *J. Neurosci.* **37**, 2686–2696 (2017).
56. Thomas, S. L. & Gorassini, M. A. Increases in Corticospinal Tract Function by Treadmill Training After Incomplete Spinal Cord Injury. *Journal of Neurophysiology* **94**, 2844–2855 (2005).
57. Potter-Baker, K. A. *et al.* Reliability of TMS metrics in patients with chronic incomplete spinal cord injury. *Spinal Cord* **54**, 980–990 (2016).
58. Iyer, P. C. & Madhavan, S. Characterization of stimulus response curves obtained with transcranial magnetic stimulation from bilateral tibialis anterior muscles post stroke. *Neuroscience Letters* **713**, 134530 (2019).
59. Hassanzahraee, M., Zoghi, M. & Jaberzadeh, S. Longer Transcranial Magnetic Stimulation Intertrial Interval Increases Size, Reduces Variability, and Improves the Reliability of Motor Evoked Potentials. *Brain Connectivity* **9**, 770–776 (2019).
60. Reisman, D. S., Block, H. J. & Bastian, A. J. Interlimb Coordination During Locomotion: What Can be Adapted and Stored? *Journal of Neurophysiology* **94**, 2403–2415 (2005).
61. Kim, H. E., Corcos, D. M. & Hornby, T. G. Increased spinal reflex excitability is associated with enhanced central activation during voluntary lengthening contractions in human spinal cord injury. *Journal of Neurophysiology* **114**, 427–439 (2015).
62. Billot, M., Duclay, J., Rigoard, P., David, R. & Martin, A. Antagonist muscle torque at the ankle interfere with maximal voluntary contraction under isometric and anisometric conditions. *Sci Rep* **12**, 20238 (2022).
63. Kesar, T. M. *et al.* Agonist-Antagonist Coactivation Enhances Corticomotor Excitability of Ankle Muscles. *Neural Plasticity* **2019**, 1–12 (2019).

64. Jayaraman, A. *et al.* Locomotor Training and Muscle Function After Incomplete Spinal Cord Injury: Case Series. *The Journal of Spinal Cord Medicine* **31**, 185–193 (2007).
65. Zewdie, E. T., Roy, F. D., Yang, J. F. & Gorassini, M. A. Facilitation of descending excitatory and spinal inhibitory networks from training of endurance and precision walking in participants with incomplete spinal cord injury. in *Progress in Brain Research* vol. 218 127–155 (Elsevier, 2015).
66. Gottschall, J. S. & Kram, R. Energy cost and muscular activity required for propulsion during walking. *Journal of Applied Physiology* **94**, 1766–1772 (2003).
67. Huang, H. J., Kram, R. & Ahmed, A. A. Reduction of Metabolic Cost during Motor Learning of Arm Reaching Dynamics. *Journal of Neuroscience* **32**, 2182–2190 (2012).
68. Diehl, Ph., Kliesch, U., Dietz, V. & Curt, A. Impaired facilitation of motor evoked potentials in incomplete spinal cord injury. *J Neurol* **253**, 51–57 (2006).
69. Kemlin, C. *et al.* Redundancy Among Parameters Describing the Input-Output Relation of Motor Evoked Potentials in Healthy Subjects and Stroke Patients. *Front. Neurol.* **10**, 535 (2019).
70. Devanne, H., Lavoie, B. A. & Capaday, C. Input-output properties and gain changes in the human corticospinal pathway: *Exp Brain Res* **114**, 329–338 (1997).
71. Carroll, T. J., Riek, S. & Carson, R. G. Reliability of the input–output properties of the cortico-spinal pathway obtained from transcranial magnetic and electrical stimulation. *Journal of Neuroscience Methods* **112**, 193–202 (2001).
72. Karakasis, C. & Artemiadis, P. Real-time kinematic-based detection of foot-strike during walking. *Journal of Biomechanics* **129**, 110849 (2021).
73. Buurke, T. J. W. *et al.* Split-belt walking: An experience that is hard to forget. *Gait & Posture* **97**, 184–187 (2022).
74. Stenum, J. & Choi, J. T. Step time asymmetry but not step length asymmetry is adapted to optimize energy cost of split-belt treadmill walking. *J Physiol* **598**, 4063–4078 (2020).
75. Malone, L. A., Bastian, A. J. & Torres-Oviedo, G. How does the motor system correct for errors in time and space during locomotor adaptation? *Journal of Neurophysiology* **108**, 672–683 (2012).
76. Leech, K. A., Roemmich, R. T. & Bastian, A. J. Creating flexible motor memories in human walking. *Sci Rep* **8**, 94 (2018).
77. Ogawa, T., Kawashima, N., Obata, H., Kanosue, K. & Nakazawa, K. Mode-dependent control of human walking and running as revealed by split-belt locomotor adaptation. *Journal of Experimental Biology* jeb.120865 (2015) doi:10.1242/jeb.120865.
78. Péronnet, F. & Massicotte, D. Table of nonprotein respiratory quotient: an update. *Can J Sport Sci* **16**, 23–29 (1991).
79. Sánchez, N., Park, S. & Finley, J. M. Evidence of Energetic Optimization during Adaptation Differs for Metabolic, Mechanical, and Perceptual Estimates of Energetic Cost. *Sci Rep* **7**, 7682 (2017).

Acknowledgments

This study was funded by the University of Colorado Anschutz-Boulder Nexus grant and the NIH National Center of Neuromodulation for Rehabilitation (P2CHD086844). ACS was supported by the Eunice Kennedy Shriver National Institute of Child Health and Human Development of the National Institutes of Health (K01HD106928) and the Boettcher Foundation’s Webb-Waring Biomedical Research Program. We would like to

thank our study participants and our collaborators at the University of Colorado, Anschutz Medical Campus.

Author contributions statement

A.T.B., T.G.H., A.C.S., and A.Q.T. contributed to the conception and design of the study; A.T.B., T.G.H., and A.K.P. conducted the experiments; A.T.B. and T.G.H. analyzed the data; A.T.B. and T.G.H. drafted the original manuscript; all authors contributed to the interpretation of the results and revisions of the manuscript; All authors approved the final version of the manuscript.

Additional information

The authors declare no competing financial interests.

Data availability

The authors confirm that the data supporting the findings of this study are fully available and presented in the supporting information of the manuscript. Correspondence and requests for materials should be addressed to A.Q.T.

Display items

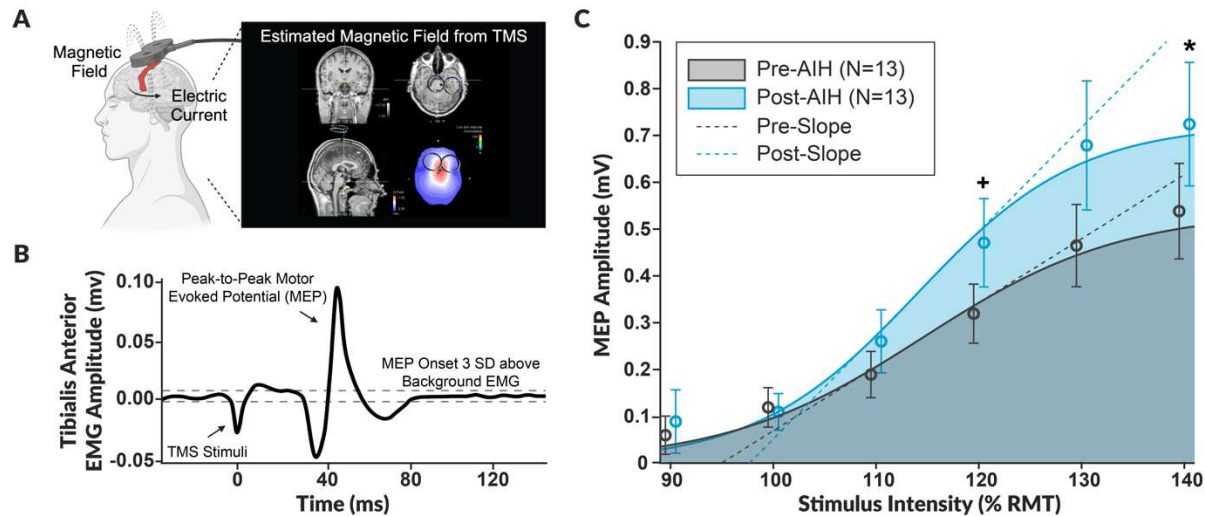


Figure 1. The average transcranial magnetic stimulation recruitment curve pre- and post-acute intermittent hypoxia exposure. **A.** We used single-pulse transcranial magnetic stimulation (TMS) to assess changes in corticospinal excitability to the tibialis anterior before and after five consecutive days of acute intermittent hypoxia (AIH). We applied TMS over the scalp to target the lower limb motor area of the primary motor cortex. We utilized a neuronavigational system to ensure trial-to-trial consistency in the stimulation vector. The hotspot corresponded to the location that elicited the lowest threshold and shortest latency motor evoked potential (MEP) amplitude. **B.** The MEP was recorded using surface electromyography (EMG) placed over the tibialis anterior muscle belly. We utilized the peak-to-peak MEP amplitude as an index to evaluate changes in corticospinal excitability, where the onset was identified as the first frame to exceed three standard deviations of the pre-stimulus background EMG. **C.** The average recruitment curve for thirteen participants was generated by plotting the peak-to-peak MEP amplitude versus the normalized stimulus intensity based on 90% to 140% of the participants' resting motor threshold (RMT) pre-AIH (grey) and post-AIH (blue). The dashed line represents the Boltzmann slope, the shaded area depicts the area under the curve, and the bars represent standard error. The significance levels of an ANOVA comparing pre-AIH and post-AIH at the stimulus intensities of 100% RMT, 120% RMT, and 140% RMT are denoted as * $p < 0.05$ and + $p = 0.05$.

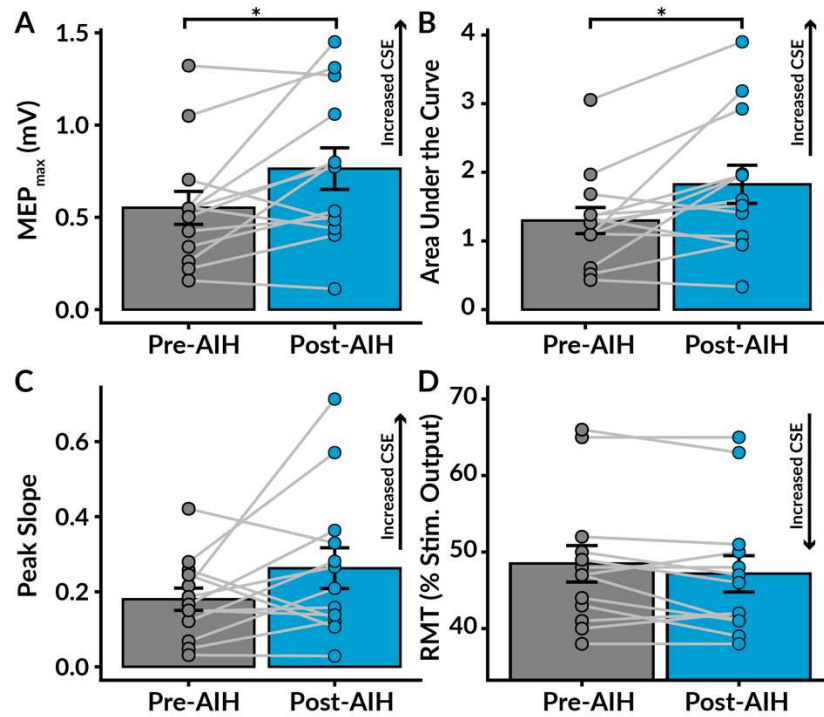


Figure 2. Average corticospinal excitability pre- and post-acute intermittent hypoxia exposure. We evaluated changes in corticospinal excitability (CSE) pre- to post-acute intermittent hypoxia (AIH) by measuring alterations in the maximum motor evoked potential amplitude (MEP_{max}), area under the recruitment curve, peak slope of the recruitment curve, and resting motor threshold (RMT; as a percent of the maximal stimulator output). **A.** The average MEP_{max} significantly increased following AIH, indicating increased CSE. **B.** The area under the recruitment curve, an index of net excitability from 90% to 140% of RMT, also significantly increased post-AIH. **C.** There was no significant change in peak slope after AIH. **D.** The RMT decreased after AIH, suggesting increased CSE. However, this change only approached significance ($p = 0.088$). The bars represent standard error. Significance levels are denoted as *** $p < 0.001$, ** $p < 0.01$, and * $p < 0.05$.

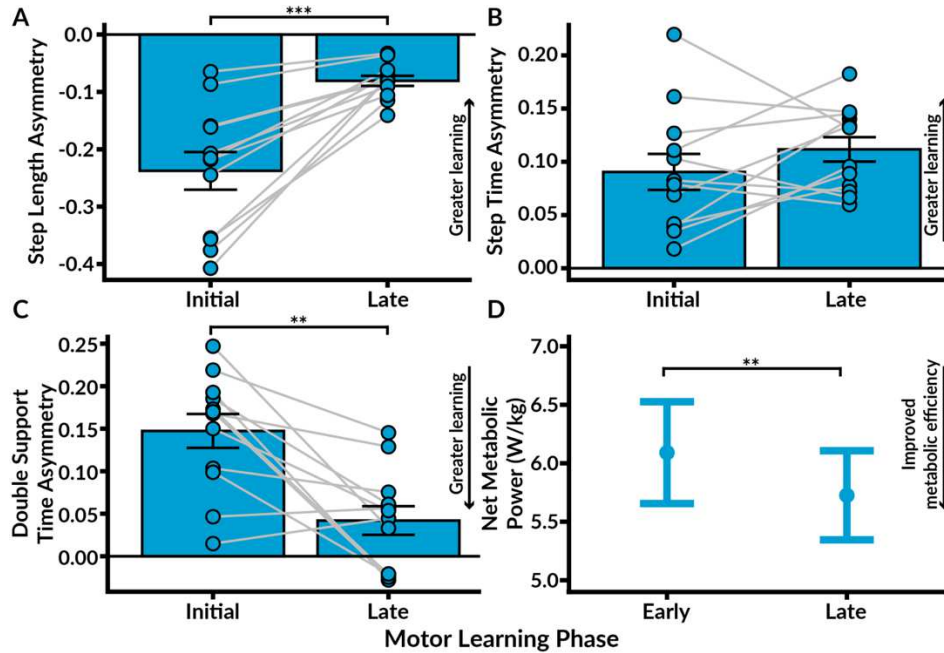


Figure 3. Motor Learning: Spatiotemporal and metabolic adaptation during the first exposure to split-belt walking. We quantified motor learning by measuring the extent of spatiotemporal adaptation from the first five strides ('initial') to the final twenty strides ('late') of the first exposure to split-belt walking ('Adapt 1'). Additionally, we assessed the magnitude of metabolic adaptation by comparing the second minute ('early') of Adapt 1 to the last minute ('late'). **A.** We observed substantial reductions in step length asymmetry during Adapt 1, indicating spatial motor learning. **B.** In contrast, step time asymmetry remained high without significant changes. **C.** Double support time asymmetry significantly decreased from initial Adapt 1 to late Adapt 1, consistent with temporal motor learning. **D.** Net metabolic power significantly reduced during Adapt 1, suggesting improved metabolic efficiency. The circles and light grey lines depict individual data. The bars represent standard error. Significance levels are denoted as *** $p < 0.001$, ** $p < 0.01$, and * $p < 0.05$.

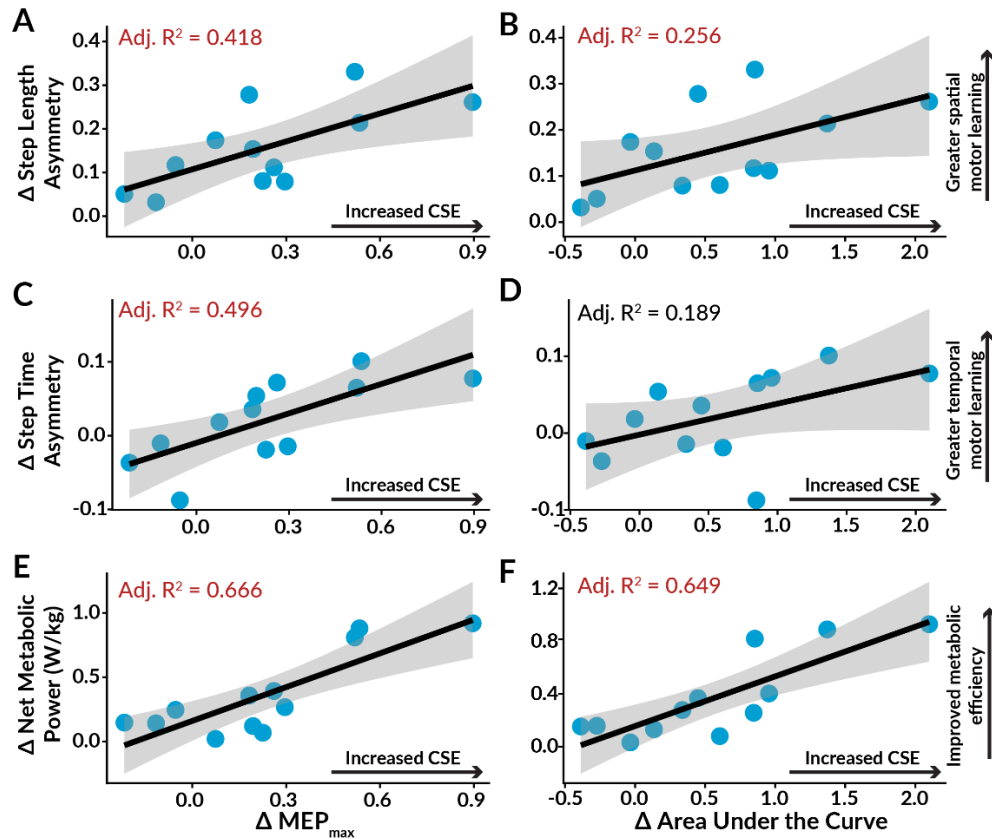


Figure 4. Linear regressions among TMS indices of AIH-induced enhancements in corticospinal excitability and their correlation with motor learning outcomes. The red text indicates statistically significant adjusted R^2 values ($p < 0.05$), while the black text signifies insignificant values. **A.** We observed a significant positive correlation between increased maximum motor-evoked potential amplitude (MEP_{max}) post-AIH and improvements in step length asymmetry during Adapt 1. **B.** The association between elevated area under the recruitment curve post-AIH and enhanced step length asymmetry during motor learning approached significance ($p = 0.053$). **C.** We identified a significant correlation between elevated MEP_{max} post-AIH and augmented step time asymmetry during Adapt 1. **D.** Correlations between increased area under the recruitment curve post-AIH and greater step time asymmetry during motor learning approached significance ($p = 0.088$). **E.** Elevated MEP_{max} after AIH exhibited a positive correlation with decreased net metabolic power during motor learning. **F.** Heightened area under the recruitment curve post-AIH positively correlated with reduced net metabolic power during Adapt 1. Individual data points are represented in blue, and the 95% confidence interval is illustrated by the grey-shaded area.

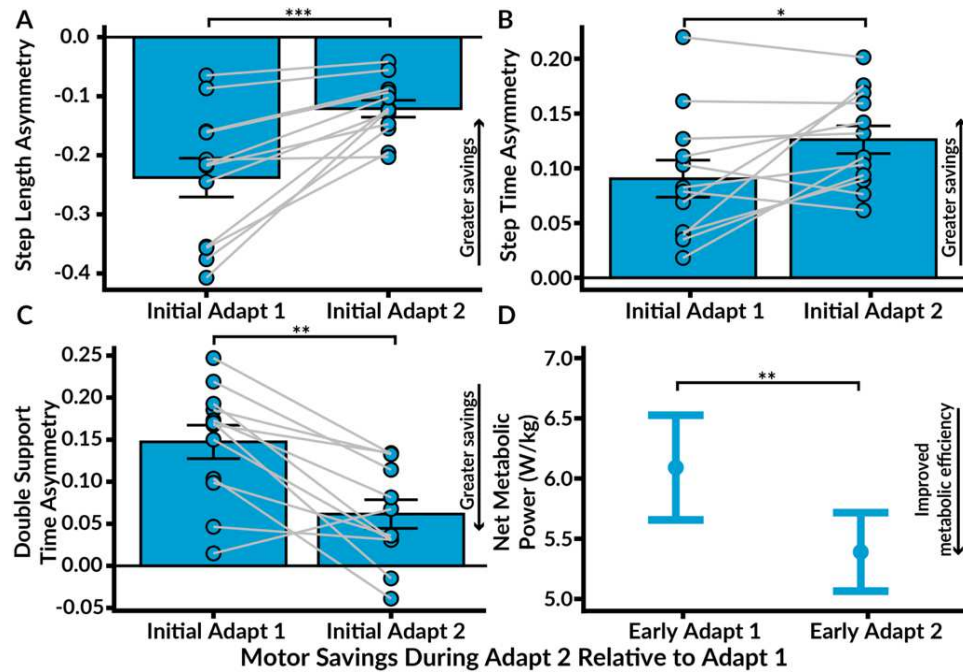


Figure 5. Motor Savings. We characterized motor savings by measuring the degree of spatiotemporal adaptation from initial Adapt 1 to initial Adapt 2 and the extent of metabolic adaptation from early Adapt 1 to early Adapt 2. **A.** Savings of step length asymmetry were evidenced by significantly lower asymmetry during initial Adapt 2 relative to initial Adapt 1. **B.** Step time asymmetry was significantly elevated during initial Adapt 2 compared to initial Adapt 1. **C.** Savings of double support time asymmetry were observed, as asymmetry was significantly lower during initial Adapt 2 compared to initial Adapt 1. **D.** Savings of improved metabolic efficiency were also shown by lower net metabolic power during Adapt 2 compared to Adapt 1. The bars represent standard error. Significance levels are denoted as *** $p < 0.001$, ** $p < 0.01$, and * $p < 0.05$.

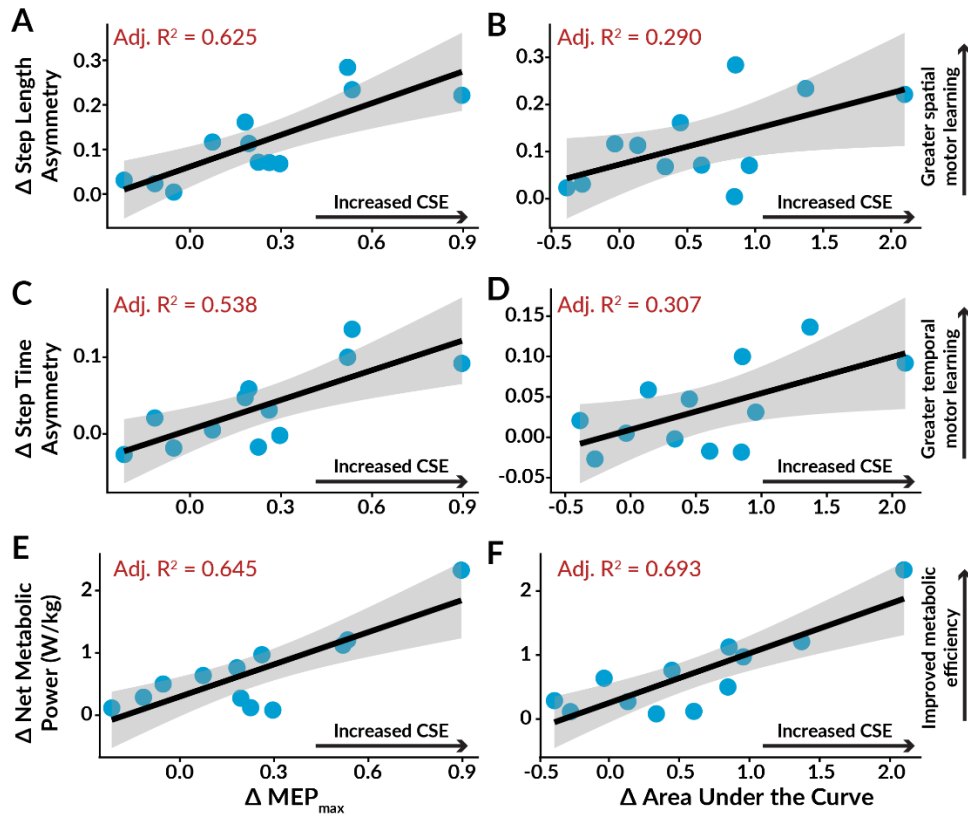


Figure 6. Linear regressions among indices of AIH-induced enhancements in corticospinal excitability and their correlation with motor savings outcomes. The red text indicates statistically significant adjusted R^2 values ($p < 0.05$), while the black text signifies insignificant values. **A.** We identified a significant correlation between increased maximum motor-evoked potential amplitude (MEP_{max}) after AIH and savings of lower step length asymmetry. **B.** Increased area under the recruitment curve post-AIH exhibited a significant correlation with the savings of lower step length asymmetry. **C.** We observed a significant correlation between heightened MEP_{max} post-AIH and the savings of higher step time asymmetry. **D.** Increased area under the recruitment curve post-AIH positively correlated with the savings of higher step time asymmetry. **E.** There was a significant correlation between elevated MEP_{max} after AIH and the savings of lower net metabolic power. **F.** We found a positive correlation between a larger area under the recruitment curve post-AIH and the savings of lower net metabolic power. Individual data points are shown in blue, and the 95% confidence interval is represented by the grey-shaded area.

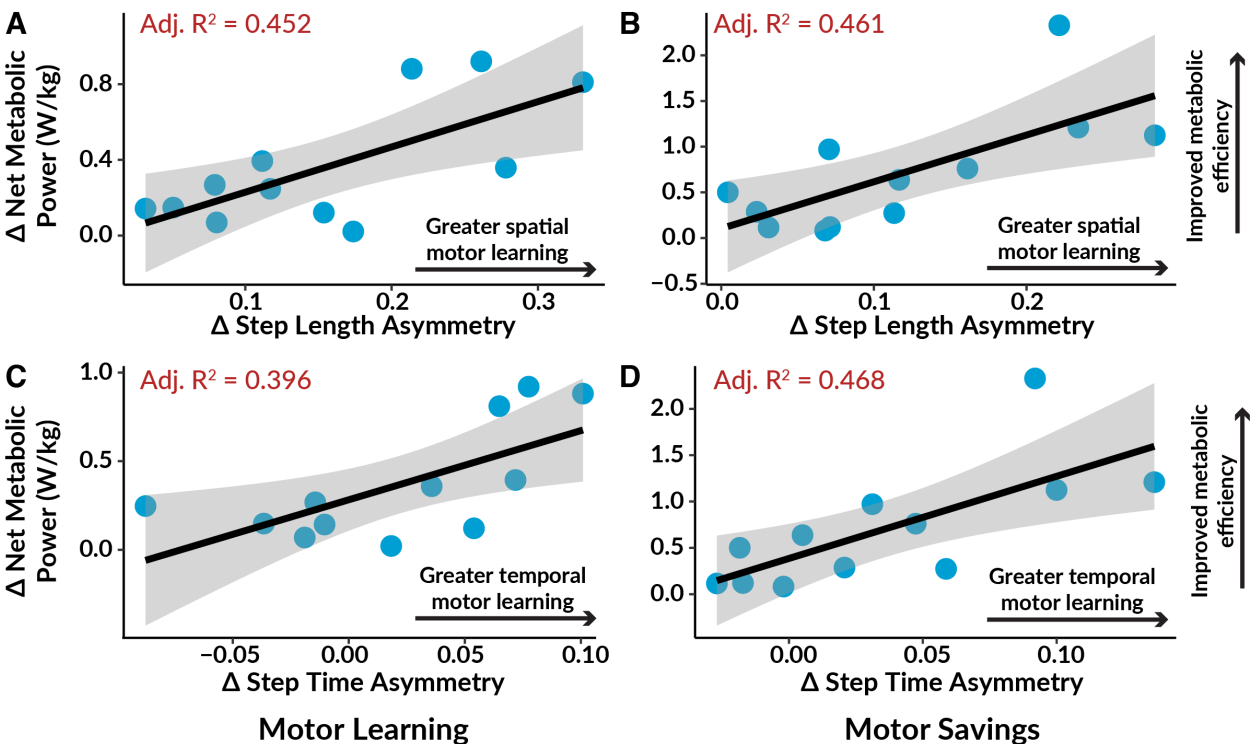
	Motor Learning	Adjusted R²	P-value
Δ MEP_{max}	Step Length Asymmetry	0.418	0.014*
	Step Time Asymmetry	0.496	0.006**
	Double Support Time Asymmetry	-0.035	0.446
	Net Metabolic Power	0.666	0.001**
Δ Area Under the Curve	Step Length Asymmetry	0.256	0.053
	Step Time Asymmetry	0.189	0.088
	Double Support Time Asymmetry	-0.067	0.591
	Net Metabolic Power	0.649	0.001**
Δ Peak Slope	Step Length Asymmetry	-0.007	0.358
	Step Time Asymmetry	0.233	0.064
	Double Support Time Asymmetry	-0.046	0.488
	Net Metabolic Power	0.313	0.034*
Δ Resting Motor Threshold	Step Length Asymmetry	-0.022	0.403
	Step Time Asymmetry	0.056	0.228
	Double Support Time Asymmetry	-0.099	0.942
	Net Metabolic Power	0.204	0.079

Table 1. Summary of the linear regression analyses performed between indices of AIH-induced enhancements in corticospinal excitability and motor learning outcomes. We performed linear regression analyses and calculated adjusted R² values to examine the correlation between transcranial magnetic stimulation indices of corticospinal excitability and motor learning outcomes. Significance levels are denoted as *** p < 0.001, ** p < 0.01, and * p < 0.05.

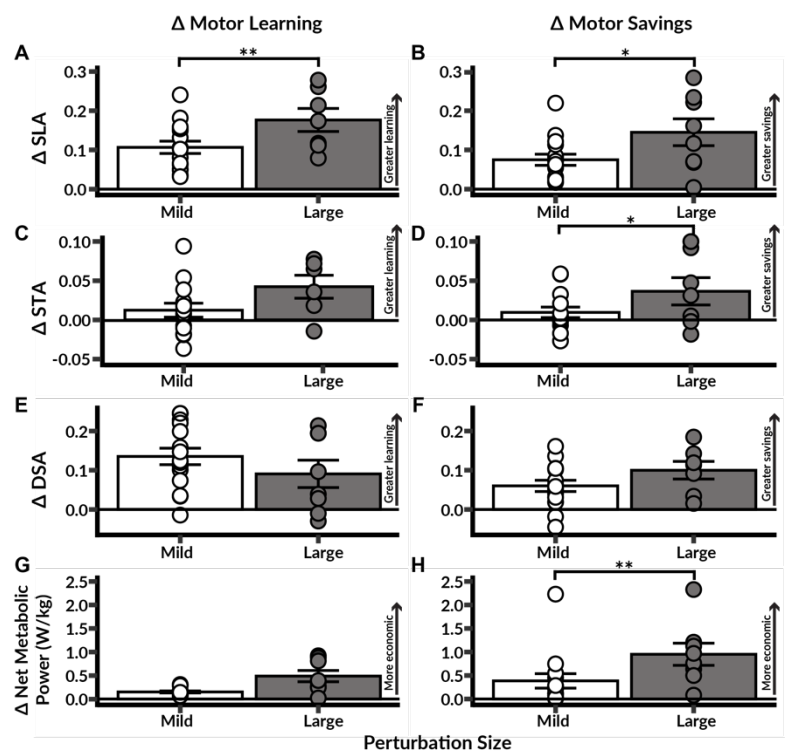
	Motor Savings	Adjusted R²	P-value
Δ MEP_{max}	Step Length Asymmetry	0.625	0.001**
	Step Time Asymmetry	0.538	0.004**
	Double Support Time Asymmetry	-0.030	0.429
	Net Metabolic Power	0.645	0.001**
Δ Area Under the Curve	Step Length Asymmetry	0.290	0.041*
	Step Time Asymmetry	0.307	0.036*
	Double Support Time Asymmetry	-0.100	0.997
	Net Metabolic Power	0.693	<0.001***
Δ Peak Slope	Step Length Asymmetry	0.090	0.179
	Step Time Asymmetry	0.119	0.146
	Double Support Time Asymmetry	-0.041	0.468
	Net Metabolic Power	0.406	0.015*
Δ Resting Motor Threshold	Step Length Asymmetry	0.019	0.296
	Step Time Asymmetry	0.031	0.272
	Double Support Time Asymmetry	0.060	0.221
	Net Metabolic Power	0.231	0.065

Table 2. Summary of the linear regression analyses performed between indices of AIH-induced enhancements in corticospinal excitability and motor savings outcomes. We conducted linear regression analyses and computed adjusted R² values to assess the relationship between transcranial magnetic stimulation indices of corticospinal excitability and motor savings outcomes. Significance levels are denoted as *** p < 0.001, ** p < 0.01, and * p < 0.05.

Supplementary information



Supplementary Figure S1. Linear regressions among indices of spatiotemporal adaptation and their correlation with changes in net metabolic power. The red text indicates statistically significant adjusted R^2 values ($p < 0.05$). **A.** We observed a significant positive correlation between the decline in step length asymmetry during motor learning and the corresponding decrease in net metabolic power. **B.** The savings of reduced step length asymmetry demonstrated a significant correlation with the savings of lower net metabolic power. **C.** We observed a significant correlation between higher step time asymmetry during motor learning and decreased net metabolic power. **D.** The savings of step time asymmetry positively correlated with the savings of reduced net metabolic power. Individual data points are shown in blue, and the 95% confidence interval is represented by the grey-shaded area.



1044 **Supplementary Figure S2. Comparison of motor learning and motor savings**
1045 **between a mild and large perturbation group.** We examined differences in motor
1046 learning (left) and motor savings (right) between a mild perturbation documented in
1047 Bogard et al., 2023 (1:1.5 belt speed ratio; white) and a large perturbation (1:2 belt speed
1048 ratio; grey). **A.** The large perturbation group displayed greater spatial motor learning than
1049 the mild perturbation group, as shown by larger reductions in step length asymmetry
1050 (SLA). **B.** The large perturbation group exhibited greater savings of lower SLA than the
1051 mild perturbation group. **C.** Both groups demonstrated an increase in step time
1052 asymmetry (STA) during motor learning. **D.** The large perturbation group showed greater
1053 savings of elevated STA compared to the mild perturbation group. **E.** Both groups
1054 adapted to reduce double support time asymmetry (DSA) during motor learning. **F.** Both
1055 groups demonstrated similar savings of lower DSA. **G.** Mean net metabolic power
1056 decreased during motor learning for both groups. **H.** The large perturbation group had
1057 greater reductions in net metabolic power from Adapt 1 to Adapt 2 compared to the mild
1058 perturbation group. The circles represent individual data. The bars indicate standard
1059 error. Significance levels are denoted as *** p < 0.001, ** p < 0.01, and * p < 0.05.

	Linear Mixed Model ANOVA			Tukey's <i>Post Hoc</i> Analyses	
	Perturbation Size	Adaptation Period	Perturbation Size x Adaptation Period	Δ Motor Learning	Δ Motor Savings
Δ Step Length Asymmetry	F(1, 21) = 6.70 p = 0.017*	F(1, 21) = 37.28 p < 0.001***	F(1, 21) = 1.98 p = 0.174	t(23.01) = -2.83 p = 0.010*	t(23.01) = -2.23 p = 0.036*
Δ Step Time Asymmetry	F(1, 21) = 3.63 p = 0.071	F(1, 21) = 1.78 p = 0.196	F(1, 21) = 2.54 p = 0.126	t(24.46) = -1.39 p = 0.178	t(24.46) = -2.27 p = 0.032*
Δ Double Support Time Asymmetry	F(1, 21) = 0.15 p = 0.705	F(1, 21) = 9.64 p = 0.005**	F(1, 21) = 5.70 p = 0.026*	t(29.05) = -1.32 p = 0.196	t(29.05) = 0.62 p = 0.538
Δ Net Metabolic Power (W/kg)	F(1, 20) = 7.51 p = 0.013*	F(1, 20) = 9.95 p = 0.005**	F(1, 20) = 0.95 p = 0.342	t(32.08) = -1.73 p = 0.093	t(32.08) = -2.82 p = 0.008**

Supplementary Table S3. Retrospective comparisons between a mild vs. large perturbation size. Linear mixed model ANOVAs were used to assess a main effect of perturbation size (i.e., mild vs. large) and adaptation period (i.e., motor learning vs. motor savings), as well as an interaction between perturbation size and adaptation period (perturbation size x adaptation period). Tukey's post hoc analyses were used to assess significant perturbation size effects. Significance levels are denoted as *** p < 0.001, ** p < 0.01, and * p < 0.05.

Participant	Age (years)	Sex	Weight (kg)	Height (cm)
1	24	M	76.82	177.80
2	27	M	86.18	170.18
3	26	M	99.79	180.34
4	24	M	73.00	180.00
5	24	F	63.00	177.00
6	23	F	76.36	165.10
7	22	F	56.82	162.56
8	22	M	103.42	193.04
9	24	F	54.88	162.56
10	20	F	52.16	162.56
11	22	M	82.10	185.42
12	24	F	64.86	167.64
13	22	F	54.43	167.64

Supplementary Table S4. Demographic characteristics of the study participants.

Thirteen able-bodied participants received AIH for 5 consecutive days at the University of Colorado, Boulder. All participants provided informed consent and had no prior history of cardiovascular disease, pulmonary complications, pain, syncope, or altitude sensitivity. All participants were recreationally active and were not undergoing physical therapy at the time of the study.